The Cryosphere Discuss., doi:10.5194/tc-2017-53, 2017
Manuscript under review for journal The Cryosphere
Discussion started: 3 April 2017

The Cryosphere Discussions
Open Access
EGU

Ice shelf fracture parameterization in an ice sheet model

Sainan Sun[1], Stephen Cornford[2], Rupert Gladstone[3], Liyun Zhao[1], John C. Moore[1,3]

[1]College of Global Change and Earth System Science, Beijing Normal University, 100082, China

[2]Department of Geography, College of Science, Swansea University, Singleton Park, Swansea, SA2 8PP, UK

[3]Arctic Centre, University of Lapland, Rovaniemi, 96101, Finland

Correspondence to: john.moore.bnu@gmail.com

Abstract. Floating ice shelves exert a stabilizing force onto the inland ice sheet. However, this buttressing effect is diminished by the fracture process, which on large scales effectively softens the ice, accelerating its flow, increasing calving, and potentially leading to ice shelf breakup. Here, we explore how the application of a continuum damage model (CDM) to the prognostic ice sheet model BISICLES can account for the effects of fracture processes on viscous ice dynamics. Damage is created by the local stress field and advects downstream. This continuum damage model is coupled to the dynamical ice flow model by decreasing the effective viscosity proportional to the damage field. To evaluate the physical role of the fracture process on large-scale ice sheet dynamics and also discern the relative importance of the parameters used in the damage model, we carry out a suite of numerical experiments based on the MISMIP+ (Marine Ice Sheet Model Intercomparison Project) marine ice sheet geometry. We find that behavior of the simulated marine ice sheet is sensitive to fracture processes on the ice shelf. In the case of a geometry that produces strong lateral stress, the stiffness of ice around the grounding line is essential to ice sheet evolution, with softer or more damaged ice leading to thinning and grounding line retreat.

1 Introduction

The largest uncertainties in sea level rise prediction are the dynamic ice sheet contributions (Jevrejeva et al., 2016). Two recent ice sheet model studies came to startling different conclusions regarding the Antarctic contributions to 21st and 22nd century sea level rise: Ritz et al. (2015) concluded that Antarctic contributions of a meter or more are implausible, whereas DeConto and Pollard (2016) find that not only is this plausible, but should even be considered likely if the former underappreciated hydrofracturing process is included and linked to climate dynamics. Observations show an increased rate of ice discharge from Greenland and Antarctica recent decades (Shepherd et al., 2012). Calving is directly responsible for a mass loss comparable to that from ice shelf basal melting (Rignot et al., 2010; Depoorter et al., 2013; Liu et al., 2014). Furthermore, increased rates of

calving and basal melt seem intertwined and act in concert to enhance mass loss from ice shelves that are in negative mass balance under present climate (Liu et al., 2014; Åström et al., 2014). Mass loss from ice shelves does not contribute to sea level rise directly, but via the restraint ice shelves apply to the ice discharge from inland to ocean across the grounding line; hence mass loss from ice shelves is expected to weaken their buttressing effect. Fürst et al. (2016) show that ice shelves in the Amundsen and Bellingshausen seas are extremely sensitive to calving, meaning that even small amount of increased calving will trigger essential dynamical responses to raise sea level. Thus to better predict the future evolution of the ice sheets, processes related to calving should be better understood and described.

Calving events originate from micro-scale cracks (Kachanov, 1999), which appear when viscous strain is too high. On microscopic scales fracturing is a discrete process which operates on time scales determined by the speed of sound in ice, far faster than the viscous processes typical of ice sheet flow. Combining these processes in a single model presents very difficult numerical challenges that have only been attempted for a few cases using discrete element models (Bassis and Jacobs, 2013; Åström et al., 2013; Åström et al., 2014). This discrete approach has a firm basis in physics with, for example, Glen's flow law emerging naturally. On macroscopic scales, the development of cracks may be seen as a statistically continuum and long-term process. The net effect is to soften ice, and hence potentially accelerate ice flow. Fractures form as the damage effect accumulates. Propagation and penetration of fractures magnify calving events. Previous continuum studies of calving fall into two main categories, but all of them are essentially empirical rather than being based on fundamental fracture process physics. The first approach treats calving as a result of macro-scale crevasses. Some of these methods are based on calculation of crevasse depth (Weertman, 1973). The crevasse depth depends on the stress field (Nye, 1957) and calving rate increases with imbalance of forces (Benn et al., 2007). The model of Nick et al. (2010) takes basal crevasses into consideration as well as surface crevassing and combines an empirical criterion for calving. Models of this category successfully reconstruct the calving rate of some individual glaciers (Nick et al., 2010; Nick et al., 2013; Cook et al., 2014), however, they compute crevasse depth based on instantaneous fields, hence could not account for the stress history on the development of fractures. Models in the second category are named Continuum Damage Mechanics (CDM), which treat calving as a continuum process that develops from micro-scale cracks to macro-scale crevasses, and damage has effect on viscous behavior of ice flow (Pralong and Funk, 2005; Duddu and Waisman, 2012; Borstad et al., 2012; Albrecht and Levermann, 2014; Krug et al., 2014). The models discussed above have reasonably successfully reproduced the calving rate and fracture distribution on some individual glaciers. Here we propose a continuum damage model (CDM) which takes into account the accumulation of damage during the ice flow as well as local sources of damage. The local source of damage comes from the stress field, water depth in crevasses and mass loss or gain from the glacier surface and bottom. The development of damage has an impact on ice viscosity, and therefore influences the evolution of ice flow through Glen's flow law, and provides a feedback to the damage field itself.

The Cryosphere Discuss., doi:10.5194/tc-2017-53, 2017
Manuscript under review for journal The Cryosphere
Discussion started: 3 April 2017

We use the state of art adaptive mesh refinement model, BISICLES (Cornford et al., 2013), as our ice flow model, and add the CDM to it. The performance of the CDM is tested on the MISMIP+ (Marine Ice Sheet Model Intercomparison Projects) experiments (Asay-Davis et al., 2016). The scheme is based on an idealized marine ice sheet geometry that has strong lateral stress gradients (Gudmundsson et al., 2012). Simulations under different ocean forced melt rates with the coupled model are compared to the ice flow model without the CDM. Through the simulations, we answer the following questions: How does damage influence the evolution of ice sheet, such as the speed and behavior of grounding line, and the ice flow velocity field? How does the geometry of the damage field affect the dynamic response to ocean forcing?

In the next Section, we describe the physics used in this study, including the CDM and ice flow model. Then we present in Section 3 a suite of experiments based on MISMIP+ to evaluate the model performance and the effect of damage on ice sheet evolution. We present the results in Section 4 and a discussion in Section 5.

2Model Description

2.1 Ice flow governing equations

We implemented the damage model in the marine ice sheet model BISICLES (Cornford et al., 2013). Ice flow velocity is computed by solving a vertically-integrated stress balance equation, in this case the Shallow-Shelf approximation of the Stokes equations (MacAyeal et al., 1996). This ice dynamics formulation performs well in ice shelves and fast-flowing ice stream simulations. Floating ice is assumed to be in hydrostatic equilibrium, so given bed elevation b and ice thickness h, surface elevation s is

$$s = max\left(h + b, \left(1 - \frac{\rho_i}{\rho_w}\right)h\right), \quad (1)$$

where $\rho_i = 910\ kg\ m^{-3}$and $\rho_w = 1028\ kg\ m^{-3}$ are densities of ice and ocean water.

Ice thickness h and horizontal velocity $\boldsymbol{u}$ satisfy the mass conservation equation

$$\frac{\partial h}{\partial t} + \nabla \cdot [\boldsymbol{u}h] = a - M \quad (2)$$

and two dimensional stress-balance equation

$$\nabla \cdot [h\bar{\mu}(2\dot{\boldsymbol{\epsilon}} + 2tr(\dot{\boldsymbol{\epsilon}})I)] + \tau^b = \rho_i g h \nabla s \quad (3)$$

together with lateral boundary conditions. In equation (2), a is the surface ice mass accumulation and M is basal melt rate of the ice shelf. In equation (3), $\dot{\boldsymbol{\epsilon}}$ is the horizontal strain rate tensor and tr is the trace operator,

$$\dot{\boldsymbol{\epsilon}} = \frac{1}{2}[\nabla \boldsymbol{u} + (\nabla \boldsymbol{u})^T], \quad (4)$$

The Cryosphere Discuss., doi:10.5194/tc-2017-53, 2017
Manuscript under review for journal The Cryosphere
Discussion started: 3 April 2017

I is the identity tensor and τ^b is the basal friction. Basal friction is computed according to Tsai et al. (2015), defined as obeying a power law far upstream inland from the grounding line, transformed into a Coulomb friction law near the grounding line. $h\bar{\mu}$ is the vertically integrated effective viscosity, which would conventionally be given by Glen's law, but is modified here to include an additional damage parameter (see section 2.2).

BISICLES is constructed using the Chombo parallel AMR (Adaptive Mesh Refinement) framework, which allows us to use a non-uniform, evolving mesh during simulations. Here, we implement a three-level refinement on top of the coarse mesh (zero level) of 4 km resolution. The grid cell size is refined by a factor of 2 at each refinement level to a finest resolution of 0.5 km around the grounding line. The time step size satisfies the Courant-Friedrichs-Lewy condition everywhere, meaning for the geometry here, about 16 time steps per year.

2.2 Damage model

In CDM, we consider the material as a continuous material, and so do not take into account the effect from individual crevasses but consider their integrated effect on ice flow. CDM has been proved to be effective in some case studies (e.g., Krug et al., 2014; Borstad et al., 2012; Pralong and Funk, 2005). The damage variable D is a scalar between 0 and 1, in which 0 means ice with no damage and 1 represents fully damaged ice, meaning a high spatial density of crevasses penetrating the whole column of the ice such that the ice provides no resistance to flow, and d is the vertical integral of D. Damage enters the stress balance equation through a modification to Glen's law. The usual relationship between deviatoric stress $\boldsymbol{\tau}$ and rate-of-strain $\dot{\boldsymbol{\epsilon}}$ is:

$$2\,A\,\tau^2\boldsymbol{\tau} = \dot{\boldsymbol{\epsilon}}, \quad (5)$$

where the flow rate exponent $n = 3$, and A is a flow rate factor, which is typically temperature dependent but set to be constant here. We replace this with

$$2\,A\,\tau^2\boldsymbol{\tau} = (1 - D(\tau))^3\dot{\boldsymbol{\epsilon}}, \quad (6)$$

which – given the shallow shelf approximation – results in an expression for the vertically integrated effective viscosity,

$$2\,h\bar{\mu} = [h - d(\tau_1)]A^{-\frac{1}{3}}\dot{\epsilon}^{-\frac{2}{3}}. \quad (7)$$

A relationship between damage and the first principal stress, $d(\tau_1)$, must be specified, at which point the stress balance equation can be solved numerically for d and $\boldsymbol{u}$ together.

In the absence of advection, we could prescribe $d(\tau_1)$ by equating it to the total depth of crevasses, computed following Nye (1957), Benn et al (2007), and Nick et al (2010). The depth of a crevasse at the upper surface is:

$$d_s = \frac{\tau_1}{\rho_i g}h + \frac{\rho_w}{\rho_i}d_w, \quad (8)$$

The Cryosphere Discuss., doi:10.5194/tc-2017-53, 2017
Manuscript under review for journal The Cryosphere
Discussion started: 3 April 2017

while at the lower surface it is

$$d_b = \frac{\rho_i}{\rho_w - \rho_i}\left(\frac{\tau_1}{\rho_i g}h - h_{ab}\right), \qquad (9)$$

where d_w is the water depth in the surface crevasse and h_{ab} is the thickness above floatation. The total local crevasse depth is then $d_l = \max(d_s, d_s + d_b, 0)$.

One more modification is needed to reflect the transport of damage by ice flow. We assume that crevasse closure does not result in bonding of the crevasse surfaces, at least on the timescale of the closure itself, so that the final relationship $d(\tau_1)$ is given by

$$d(\tau_1) = max(\, d_l(\tau_1), d_{tr}\,). \qquad (10)$$

This means that regions of the ice shelf under lower stress inherit damage from any higher stress region upstream. The d_{tr} is found by solving a damage transport equation

$$\frac{\partial d_{tr}}{\partial t} + \nabla \cdot (\boldsymbol{u} d_{tr}) = -[max(a, 0) + max(-M, 0)]\frac{d_{tr}}{h}, \qquad (11)$$

We specify Dirichlet conditions d_{tr} = 0 on all inflow boundaries, while initial conditions are determined in the same way as ice thickness, that is, by evolving to a steady state, but with the additional proviso $d_{tr}(t - \Delta t) = d(t - \Delta t)$. Note that although damaged ice does not strengthen over time, the vertically averaged damage can strengthen through meteoric or marine ice accumulation, since ice thickens without an increase in d_{tr}. Eq. (11) has no explicit healing term to represent effect of overburden pressure, which will lead us to overstate the damage field. We assume it is relatively unimportant compared to crevasse opening in the largely tensile ice shelf flow fields most affected by damage in the results presented here.

3 Experimental design

We carried out a set of numerical experiments based on the third Marine Ice Sheet Model Intercomparison Project (MISMIP+, Asay-Davis et al., 2016). MISMIP+ includes a number of experiments based on an idealized marine ice sheet geometry derived from Gudmundsson (2012) and Gudmundsson (2013). In the experiments, ice flows along an 800 km long and 80 km wide submarine bedrock trough, from an ice divide at one end to an ice shelf and calving front at the other. The geometry features an ice shelf with lateral stresses that buttress upstream ice to the extent that it is possible to obtain a stable equilibrium with its grounding lines sited on a retrograde bedrock slope, that is, a slope rising in the direction of ice flow toward the ocean.

We had three questions in mind. First, although the CDM should weaken the ice shelf such that the steady state location of the grounding line would be altered for a given parameter A in the Glen's flow law, is it possible to find an alternative value A' which compensates for the damage? Note that A is not measured directly but typically tuned so that simulated ice flow

The Cryosphere Discuss., doi:10.5194/tc-2017-53, 2017
Manuscript under review for journal The Cryosphere
Discussion started: 3 April 2017

matches observations. Second, if similar grounding line steady states can be realised with or without the damage model, is the 'hidden' damage inherent in the difference between A and A'revealed in the response of the ice stream to thinning of the ice shelf. Third, is it necessary to evolve the damage model in time, or is it possible to simply construct a damage field at the start of a calculation and hold it constant throughout the simulation?

We investigated equilibrium states by carrying out the MISMIP+ no ocean forcing experiment (Ice0) with and without the damage model. Ice0 requires that models are close to steady state with a grounding line crossing the centre of the trough (y = 40 km) at around x = 450 km, and that they demonstrate this by showing insignificant grounding line migration over 100 years in the absence of ice shelf basal melt. Without the damage model, we set $A = 2.0 \times 10^{-17}\, Pa^{-3}\, a^{-1}$, just as in Asay-Davis et al. (2016), and found a steady state. We then switched on the damage model and ran for 1000 years to assess grounding line migration due to the weakened ice shelf. We will refer to this simulation as IceD (in general D indicates inclusion of the damage model). Then, to follow the MSIMIP+ experiments as intended, we carried out a series of experiments each running for 1000 years with a different values of A to find a value A'that resulted in an ice sheet whose grounding line was close to the original: we will refer to the test of that steady state as IceD0.

Once IceD0 had been completed, we carried out the remaining MISMIP+ experiments with the given values of A and A'. Ice1r and IceD1r see the models respond to a simple basal melt formula that concentrates ablation close to (but not at) the grounding line as it evolves over 100 years,

$$M = \frac{1}{5} tanh\left(\frac{H_c}{75.0}\right) max\big((100 - Z_d), 0\big) \quad (12)$$

where H_c is the water column thickness and Z_d is ice shelf draft. Ice1ra and IceD1ra see the ice sheet change over the next 900 years when the basal melt rate is set to zero, while Ice1rr and IceD1rr continue for the next 900 years under the influence of basal melt (eq. 12). Ice2r, IceD2r, IceD2ra, IceD2ra, Ice2rr and Ice2Drr follow the same general pattern, but impose a different melt rate

$$M = \begin{cases} 100\ m\ a^{-1}, & x \geq 480\ km \\ 0, & x < 480\ km \end{cases} \quad (13)$$

where x represent the distance away from the ice divide. This melt rate is concentrated away from the grounding line and does not evolve with it, allowing a thick ice shelf to form in the wake of a retreating grounding line. This high basal melt rate at the ice front is designed to simulate the effect of mass loss far from the grounding line on ice flux, which is an analogue to calving events in real world. Names of simulations based on different models and basal melt rates are summarized in Table 1.

Finally, we carried out versions of the Ice0, Ice1r, and Ice1ra experiments with the same A' and initial damage field as in IceD0, but without allowing the damage field to evolve over time. We will refer to these experiments as IceF0 and IceF1r, with the 'F' standing for fixed-in-time damage. This resembles realistic cases (e.g. Gong et al., 2014; Favier et al., 2015; Cornford et

The Cryosphere Discuss., doi:10.5194/tc-2017-53, 2017
Manuscript under review for journal The Cryosphere
Discussion started: 3 April 2017

al., 2015; Sun et al., 2014) where an initial damage field is estimated to match observations of velocity in the ice shelf at the start of a simulation, and held constant thereafter.

4 Results

Switching the damage model on given the steady geometry of Ice0 with A produces widespread weakening of the ice shelf, resulting in 100 km grounding line retreat. Fig. 1 shows how the damage field evolves for 1000 years from the moment the damage mechanism begins. On grounded ice the damage D is generally low, which can be attributed to both the low viscous stress and the ice overburden acting against basal crevasse formation. In the ice shelf, D is typically about $1/2$, varying from around $1/3$ close to the grounding line in the center of the channel, to nearly 1 where the grounding line crosses the channel walls. As time passes, damage is advected downstream so that strips of ice with D close to 1 extend all the way from the grounding line to the calving front. Meanwhile, the acceleration caused by this ice shelf weakening results in the grounded ice thinning and in turn the grounding line retreats, by around 70 km in the first 50 years of the simulation and a further 30 km over the full 1000 year simulation. Decreasing A to $A' = 1.5 \times 10^{-18}\, Pa^{-3}\, a^{-1}$ is sufficient to counter the damage and hold the grounding line steady at x = 450 km.

Fig. 2 shows the effective viscosity, velocity, and damage at the start of the IceD0 experiment. At this point the model is close to steady state, having been allowed to evolve for 30,000 years: neither the grounded area nor the volume above flotation changes substantially over the course of 1000 years. Just as before, ice far upstream from the grounding line is not strongly damaged, whereas D is typically around $1/2$ in the ice shelf, and larger close to the domain boundaries. It is also apparent from Fig. 2 that D begins to grow over a region a few kilometers upstream from the grounding line.

Although the pattern of damage and its impact on effective viscosity varies both laterally and between grounded and floating ice, the net effect is to produce a grounding line that is rather similar in shape and position to that of Ice0 (Fig. 3). Having established that it is possible to 'emulate' the damage model, at least in steady state, by a simple change to A, it is natural to ask if the same is true when the ice shelf is perturbed.

Fig. 4 shows the evolution of D and the grounding line location over time in the IceD1r, IceD1ra, and IceD1rr simulations. IceD1r sees the grounding line in the centre of the channel retreat from around x = 450 km to x = 390 km over the course of 100 years while the basal melt rate (eq. 12) is applied. At the same time the damage field evolves to maintain a pattern of low damage ($D << 1$) on the grounded ice and more damage ($D \sim 1/2$) in the ice shelf. Much of the ice shelf is thin ($h <$ 200 m) so that a high value of D implies only a small reduction in buttressing caused by the ice shelf. IceD1ra, which continues from IceD1r, specifies that basal melt rates return to zero, allowing the grounding line to advance toward the IceD0 steady state position by t=200. Ice in newly grounded regions has almost no damage, since the advection of damage is significantly

The Cryosphere Discuss., doi:10.5194/tc-2017-53, 2017
Manuscript under review for journal The Cryosphere
Discussion started: 3 April 2017

faster than grounding line advance. Between t=100 and t=200 years, the formerly heavily damaged region is completely lost downstream the grounding line. A tongue of less damaged ice ($D\sim 1/3$) extruds from the grounding line and a pattern akin to IceD0 (Fig. 2) is reached by t=1000. IceD1rr also follows on from IceD1r, but with basal melt rate continuously applied, driving grounding line retreat to around x = 250 km by t = 1000.

Fig. 5 plots the damage field and the grounding line during the evolution of ice in IceD2r, IceD2ra and IceD2rr experiments. The ice shelf is removed entirely beyond x = 480 km during the first 100 model years. The damage field in the remainder of the ice shelf appears much as it did in the initial state, albeit with a narrow strip of high ($D\sim 1$) damage right at the calving front. The grounding line retreats by around 20 km in the center of the channel, while the damage field evolves so that $D\sim 1/3$ immediately downstream, growing to $D\sim 1/2$ before abruptly increasing at the calving front. Experiment IceD2rr sees the same trend continue, with the grounding line retreating by a further 40 km. Experiment IceD2ra, on the other hand, exhibits a travelling front of strong damage, separating thicker ice (h > 200 m) which has been carried downstream from the ice shelf of IceD2r from ice which had been permitted to accumulate on the open sea - had such accumulation not been permitted, this damage front would have been coincident with the calving front. Over time, the original pattern of IceD0 is recovered, with $D\sim 1/3$ near the grounding line, $D\sim 1/2$ in the lateral center of the shelf for most of its length, and strips where $D\sim 1$ close to the domain boundaries.

We compare the grounded area change and ice volume change between different models and ocean forcing in Figs. 6 and 7. After tuning the parameters, our model with the CDM produces similar retreating/advancing trends to the published model results (Asay-Davis et al., 2016). For both BISICLES and BISICLES_D (BISICLES with CDM), some grounded regions become floating when we implement melt rates, and grounded area decreases gradually until the melt rates cease. The floating area could be re-grounded if melt rates were no longer applied even on the retrograde bedrock slope. Ice volume change has the same trend as grounded area. The ice volume above floatation (i.e. that can affect sea level) decreases when forced by basal melt or calving, and increases to nearly the initial state when ocean forcing disappears. In both versions of BISICLES, the ice sheet is more sensitive to basal melt near the grounding line than to extreme high basal melt representing calving at the front. However, the BISICLES_D produces less retreat under both ocean forcing scenarios.

In the experiment without basal melt, the model with fixed damage (IceF0) produces a stable ice sheet behavior similar to IceD0 and Ice0. In the experiment with high basal melt rate near the grounding line, ice behavior of the fixed damage (IceF1) ice sheet is stable and comparable to Ice1r and IceD1r (Fig. 8). For the fixed damage model, the viscosity value in the region upstream of grounding line is higher, which greatly slows down the ice flux across the grounding line. The result indicates that the viscosity around the grounding line is essential to the stability of the ice sheet.

The Cryosphere Discuss., doi:10.5194/tc-2017-53, 2017
Manuscript under review for journal The Cryosphere
Discussion started: 3 April 2017

5 Discussion

The CDM produces a plausible damage distribution on this particular MISMIP+ geometry: Damage is observed to be low on the grounded ice, while it increases dramatically when the ice crosses the grounding line and increases gradually downstream from there, (Bindschadler et al., 2011). The experiments Ice0 and IceD which show explicitly the result of adding damage to the ice shelf produced rapid grounding line retreat over the full 1000 years simulations (Fig. 1). Thus the buttressing force of the undamaged ice and its corresponding ice viscosity in the shelf is essential to the behavior of the ice sheet when using the MISMIP+ geometry.

Although the damage distribution is highly localized, we showed that by tuning the viscous parameter A in the control experiment IceD0 we can match the grounding line in steady state achieved with Ice0. The required flow law parameter is an order of magnitude greater than the MISMIP+ value of A. Simulations IceD1r, IceD1rr, IceD1ra, IceD2r, IceD2ra, and IceD2rr all exhibit similar overall trends to the unmodified BISICLES model, despite extensive spatial variation in the damage field. However the effective viscosity around the grounding line under the various experiments with and without the damage model is similar. This implies that for this geometry, the viscosity of ice around the grounding line essentially controls the grounding line position, while the state of the ice shelf far from grounding line has much less impact. The ice shelf is relatively thin (<200 m) except near the grounding line and thus contributes little buttressing to inland ice flux.

Including a CDM in a realistic simulation may, perhaps counterintuitively, result in lower sensitivity of the ice sheet to ice shelf ablation and sea level rise. Recall that, given an initial stable state with similar geometry and flow field, BISICLES_D saw lower rates of both retreat and advance in the Ice1 and Ice2 experiments than the BISICLES - especially the Ice2 experiment (Fig. 6, Fig. 7). We can attribute this to the lower value of A (more viscous ice) needed across the domain to compensate for the weaker ice shelf. Once that weaker ice shelf is removed, the remaining ice sheet tends to have a larger viscosity, certainly upstream from the grounding line, than it did in the undamaged case. Realistic simulations, as least if tuned to match observed geometry and velocity, might be expected to behave in the same way.

The relative effects on the grounding line position of experiments with 'realistic' basal melt patterns, where basal melt is highest close to the grounding line (Ice1r), and those designed to mimic calving (Ice2r), where basal melt is very high near the ice shelf edge, show that calving has much less control on grounding line retreat. This does not mean calving process is unimportant for grounding line position, because in our special geometry, the side walls apply strong back stress and the removed ice is mostly downstream of the side wall, which will not be the general case in reality for large ice shelves in particular.

The evolution of the damage field in all of the experiments can be approximated, crudely at least, by a simple rule. There is little or no damage to grounded ice, while $D \sim 1/2$ at all times in the ice shelf, unless the ice is so thin as to contribute little buttressing. Thus, in the absence of a damage model, it might be possible to emulate its effects simply by setting $D \sim 1/2$ (or

equivalently, multiplying A by ~ $1/8$, that is setting an enhancement factor E ~ 8) (Paterson, 2000). The primary cause of this simple pattern is the Nye crevasse formulae (eqns.6 and 7): basal crevasses are deep – an order of magnitude deeper than surface crevasses – when and only when ice is close to or at flotation, while in a simple model of the ice shelf, with no lateral variation, and no buttressing, it is straightforward to see that $d_b + d_s = \frac{h}{2}$, by noting that the vertically integrated stress given by the calving front boundary condition is maintained throughout the shelf. As $d_b \gg d_s$ by about a factor of 10, depending on densities, modelled damage is much higher in the shelf than on grounded ice. This is consistent with observations that large-scale crevasse-like surface features are common on the ice shelves along the Amundsen and Bellingshausen Seas and on the smaller ice shelves between the Amery and Ross ice shelves of east Antarctica (Liu et al., 2015). Ground-penetrating radar show that many of these are, in fact, the surface expression of deep and wide transverse basal crevasses (Bassis and Jacobs, 2013; McGrath, et al., 2012) or longitudinal sub-glacial melt channels (Vaughan et al., 2012), that may penetrate 200 m into the base of the ice shelf, while the surface depressions are typically 30 m lower than the usual ice shelf surface (Liu et al., 2014). Lack of healing from overburden pressure in the CDM will lead to an overstated damage field when applied to ice shelves with moderate stress environments. In that case, yield stress for healing should be considered for different conditions (Albrecht and Levermann, 2014).

In BISICLES_D, viscosity around the grounding line is reduced by the high damage value produced by the large principal stress (eqns. 6 and 7). From Fig. 8, we see the retreat of grounding line in the fixed damage model (IceF1r) is much slower than in the model with evolving damage (IceD1r) and the model without damage (Ice1r), because the grounding line retreats inland where viscosity is much higher due to lower damage compared to IceD1r and smaller A compared to Ice1r. The comparison implies that the viscosity around the grounding line has essential control on ice flux.

6 Conclusions

We developed a continuum damage mechanics model component of the BISICLES ice sheet model. The model computes the evolution of a vertically integrated damage field by generating local damage according to a modification to Glen's flow law, and transporting it downstream with the ice flow field. Although the modification to Glen's flow law is based upon the crevasse opening formulae of Nye (1957), Benn et al. (2007) and Nick et al. (2010) it can be adapted to any relationship between local stretching stress and damage.

The model was tested by carrying out the MISMIP+ (Asay-Davis et al 2016) experiments with and without the damage model. Simply introducing the damage calculation results in a much weaker ice shelf given the same flow law parameter (A), so that the grounding line retreats. However, realistic simulations tend to tune A to match observations, for example by solving an inverse problem to match velocities. We were able to produce similar steady states, defined primarily by grounding line

position, for the two models by choosing a value of A around ten times larger for the flow model with damage than for the model without. Once we had done so, the response of the ice stream to ablation of the ice shelf was rather similar in both cases, with the damage model resulting in slightly lower rates of retreat, especially when the ablation was limited to the downstream portion of the ice stream. We explain this lower rate of retreat by noting that damage is far greater in the ice shelf, which must be compensated for by stiffer ice upstream to have the same steady state: once the ice shelf is removed, we are left with the dynamics of stiffer ice. Put another way, if ice shelves are generally weaker, their loss is of lower consequence.

Acknowledgements

We thank Lionel Favier for the helpful comments on the former version of this manuscript. This study is supported by China Postdoctoral Science Foundation NO. 212400240, National Key Science Program for Global Change Research (2015CB953601), and National Natural Science Foundation of China (Nos. 41530748, 41506212).

References

Albrecht, T. and Levermann, A.: Fracture-induced softening for large-scale ice dynamics, The Cryosphere, 8, 587–605, doi:10.5194/tc-8-587-2014, 2014.

Asay-Davis, X. S., Cornford, S. L., Durand, G., Galton-Fenzi, B. K., Gladstone, R. M., Gudmundsson, G. H., Hattermann, T., Holland, D. M., Holland, D., Holland, P. R., Martin, D. F., Mathiot, P., Pattyn, F., and Seroussi, H.: Experimental design for three interrelated marine ice sheet and ocean model intercomparison projects: MISMIP v. 3 (MISMIP+), ISOMIP v.2 (ISOMIP+) and MISOMIP v.1 (MISOMIP1), Geosci. Model Dev., 9, 2471-2497, doi:10.5194/gmd-9-2471-2016, 2016.

Åström, J. A., Vallot, D., Schäfer, M., Welty, E. Z., O'Neel, S., Bartholomaus, T. C. and Moore, J. C.: Termini of calving glaciers as self-organized critical systems. Nature Geoscience, 7(12), 874-878, 2014.

Åström, J. A., Riikilä, T. I., Tallinen, T., Zwinger, T., Benn, D., Moore, J. C., and Timonen, J.: A particle based simulation model for glacier dynamics, The Cryosphere, 7, 1591–1602, doi:10.5194/tc-7-1591-2013, 2013.

Bassis, J. N. and Jacobs, S. S.: Diverse calving patterns linked to glacier geometry. Nat Geosci., 6(10), 833–836, 2013.

Benn, D. I., Hulton, N. R., and Mottram, R. H.: 'Calving laws', 'sliding laws' and the stability of tidewater glaciers, Ann. Glaciol., 46, 123–130, 2007a.

Benn, D. I., Warren, C. R., and Mottram, R. H.: Calving processes and the dynamics of calving glaciers, Earth-Sci. Rev., 82, 143–179, 2007b.

Bindschadler, R., Vaughan, D. G. and Vornberger, P.: Variability of basal melt beneath the Pine Island Glacier ice shelf, West Antarctica, J. Glaciol., 57, 585-595, 2011.

Borstad, C. P., Khazendar, A., Larour, E., Morlighem, M., Rignot, E., Schodlok, M. P., and Seroussi, H.: A damage mechanics assessment of the Larsen B ice shelf prior to collapse: Toward a physically-based calving law, Geophys. Res. Lett., 39, L18502, doi:10.1029/2012GL053317, 2012.

Cornford, S. L., Martin, D. F., Graves, D. T., Ranken, D. F., Le Brocq, A. M., Gladstone, R. M., Payne, A. J., Ng, E. G., and Lipscomb, W. H.: Adaptive mesh, finite volume modeling of marine ice sheets, J. Comput. Phys., 232, 529–549, 2013.

Cornford, S. L., Martin, D. F., Payne, A. J., Ng, E. G., Le Brocq, A. M., Gladstone, R. M., Edwards, T. L., Shannon, S. R., Agosta, C., van den Broeke, M. R., Hellmer, H. H., Krinner, G., Ligtenberg, S. R. M., Timmermann, R., and Vaughan, D. G.: Century-scale simulations of the response of the West Antarctic Ice Sheet to a warming climate, The Cryosphere, 9, 1579-1600, doi:10.5194/tc-9-1579-2015, 2015.

Cook, S., Rutt, I. C., Murray, T., Luckman, A., Zwinger, T., Selmes, N., Goldsack, A., and James, T. D.: Modelling environmental influences on calving at Helheim Glacier in eastern Greenland, The Cryosphere, 8, 827–841, doi:10.5194/tc-8-827-2014, 2014.

DeConto, R. M., & Pollard, D.: Contribution of Antarctica to past and future sea-level rise. Nature, 531(7596), 591-597, 2016.

Depoorter, M., Bamber, J., Griggs, J., Lenaerts, J., Ligtenberg, S., van den Broeke, M., and Moholdt, G.: Calving fluxes and basal melt rates of Antarctic ice shelves, Nature, 502, 82–92, 2013.

Duddu, R. and Waisman, H.: A temperature dependent creep damage model for polycrystalline ice, Mech. Mater., 46, 23–41, 2012.

Favier, L., Durand, G., Cornford, S. L., Gudmundsson, G. H., Gagliardini, O., Gillet-Chaulet, F. and Le Brocq, A. M. Retreat of Pine Island Glacier controlled by marine ice-sheet instability. Nature Climate Change, 4(2), 117-121, 2014.

Fürst, J. J., Durand, G., Gillet-chaulet, F., Tavard, L., Rankl, M., Braun, M., and Gagliardini, O.: The safety band of Antarctic ice shelves. Nature Clim. Change, 6, 2014–2017, 2016.

Gong, Y., Cornford, S. L., and Payne, A. J.: Modelling the response of the Lambert Glacier–Amery Ice Shelf system, East Antarctica, to uncertain climate forcing over the 21st and 22nd centuries, The Cryosphere, 8, 1057-1068, doi:10.5194/tc-8-1057-2014, 2014.

Gudmundsson, G. H., Krug, J., Durand, G., Favier, L., and Gagliardini, O.: The stability of grounding lines on retrograde slopes, The Cryosphere, 6, 1497–1505, doi:10.5194/tc-6-1497-2012, 2012.

Gudmundsson, G. H.: Ice-shelf buttressing and the stability of marine ice sheets, The Cryosphere, 7, 647–655, doi:10.5194/tc-7-647-2013, 2013.

Jevrejeva, S., Jackson, L. P., Riva, R. E., Grinsted, A., & Moore, J. C. (2016). Coastal sea level rise with warming above 2° C. Proceedings of the National Academy of Sciences, 201605312.

Kachanov, L.M.: Rupture time under creep conditions, Int. J. Frac. 97(1–4), 11–18, 1999.

Krug, J., Weiss, J., Gagliardini, O., & Durand, G.: Combining damage and fracture mechanics to model calving. The Cryosphere, 8(6), 2101-2117, 2014.

Liu, Y., Cheng, X., Hui, F., Wang, X., Wang, F. and Cheng, C.: Detection of crevasses over polar ice shelves using Satellite Laser Altimeter. Sci. China Earth Sci., 57, 1267-1277, 2014.

Liu, Y., Moore, J.C., Cheng, X., Gladstone, R.M., Bassis, J.N., Liu, H., Wen, J., and Hui, F.: Ocean-driven thinning enhances iceberg calving and retreat of Antarctic ice shelves PNAS, 112 (11), 3263–268, 2015.

MacAyeal, D. R.: A tutorial on the use of control methods in ice sheet modeling, J. Glaciol., 39, 91–98, 1993.

McGrath, D., K. Steffen, H. Rajaram, T. Scambos, W. Abdalati, and E. Rignot: Basal crevasses on the Larsen C Ice Shelf, Antarctica: Implications for meltwater ponding and hydrofracture, Geophys. Res. Lett., 39, L16504, doi:10.1029/2012GL052413, 2012.

Nick, F. M., van der Veen, C. J., Vieli, A., and Benn, D. I.: A physically based calving model applied to marine outlet glaciers and implications for the glacier dynamics, J. Glaciol., 56, 781–794, 2010.

Nick, F. M., Vieli, A., Andersen, M. L., Joughin, I., Payne, A., Edwards, T. L., Pattyn, F., and van de Wal, R. S.: Future sea-level rise from Greenland/'s main outlet glaciers in a warming climate, Nature, 497, 235–238, 2013.

Nye, J.F.: The distribution of stress and velocity in glaciers and ice-sheets. Proc. R. Soc. London, Ser. A, 239(1216), 113–133, 1957.

Pralong, A. and Funk, M.: Dynamic damage model of crevasse opening and application to glacier calving, J. Geophys. Res., 110, B01309, doi:10.1029/2004JB003104, 2005.

Rignot, E., Koppes, M., and Velicogna, I.: Rapid submarine melting of the calving faces of West Greenland glaciers, Nat. Geosci., 3, 187–191, 2010.

Ritz, C., Edwards, T. L., Durand, G., Payne, A. J., Peyaud, V., & Hindmarsh, R. C.: Potential sea-level rise from Antarctic ice-sheet instability constrained by observations. Nature, 528(7580), 115-118, 2015.

Shepherd, A., Ivins, E. R., Geruo, A., Barletta, V. R., Bentley, M. J., Bettadpur, S., Briggs, K. H., Bromwich, D. H., Forsberg, R., Galin, N., Horwath, M., Jacobs, S., Joughin, I., King, M. A., Lenaerts, J. T. M., Li, J., Ligtenberg, S. R. M., Luckman, A., Luthcke, S. B., McMillan, M., Meister, R., Milne, G., Mouginot, J., Muir, A., Nicolas, J. P., Paden, J., Payne, A. J., Pritchard, H., Rignot, E., Rott, H., Sandberg Sørensen, L., Scambos, T. A., Scheuchl, B., Schrama, E. J. O., Smith, B., Sundal, A. V., van Angelen, J. H., van de Berg,W. J., van den Broeke, M. R., Vaughan, D. G., Velicogna, I.,Wahr, J., Whitehouse, P. L.,Wingham, D. J., Yi, D., Young, D., and Zwally, H. J.: A reconciled estimate of ice-sheet mass balance, Science, 338, 1183–1189, 2012.

Sun, S., Cornford, S. L., Liu, Y., and Moore, J. C.: Dynamic response of Antarctic ice shelves to bedrock uncertainty. The Cryosphere, 8(4), 1561-1576, 2014.

Vaughan, D. G., Corr, H. F. J., Bindschadler, R. A., Dutrieux, P., Gudmundsson, G. H., Jenkins, A., Newman, T., Vornberger, P. and Wingham, D. J.: Subglacial melt channels and fracture in the floating part of Pine Island Glacier, Antarctica, J. Geophys. Res., 117, F03012, doi:10.1029/2012JF002360, 2012.

Weertman, J.: Can a water-filled crevasse reach the bottom surface of a glacier? IASH Publ. 95 (Symposium at Cambridge 1969 – Hydrology of Glaciers), 139–145, 1973.

The Cryosphere Discuss., doi:10.5194/tc-2017-53, 2017
Manuscript under review for journal The Cryosphere
Discussion started: 3 April 2017

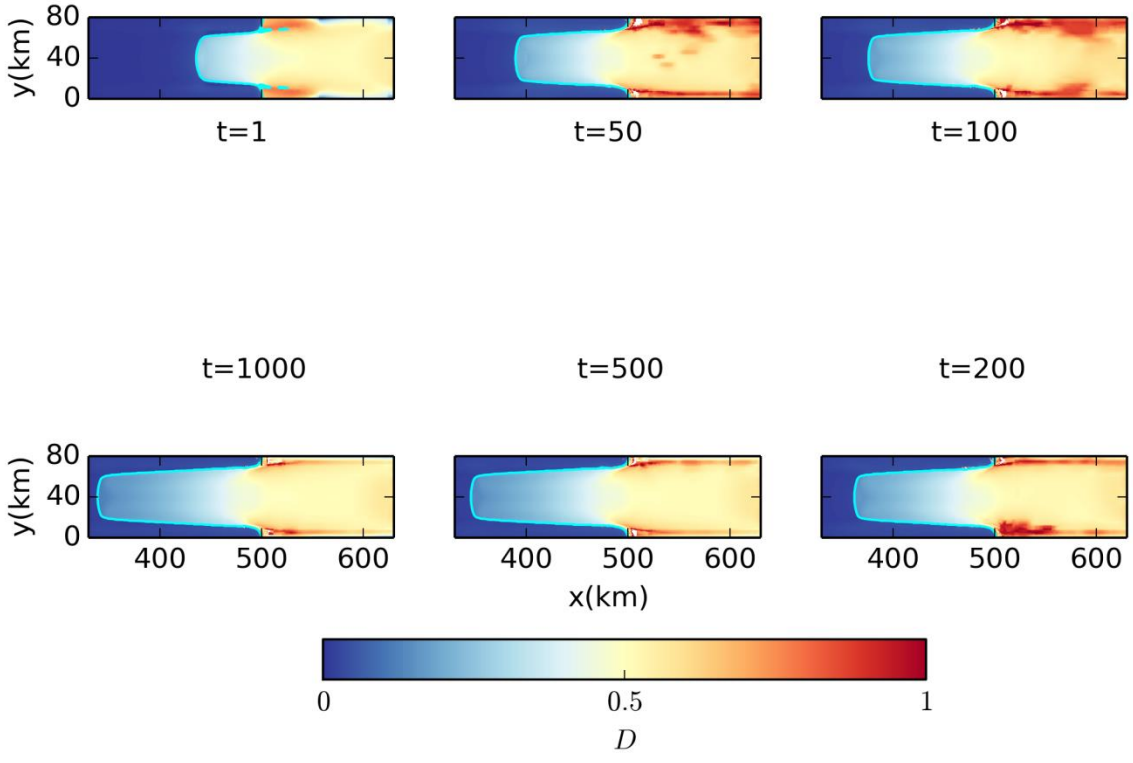

Figure 1: Evolution of the damage field D and the grounding line, starting from a steady state with $D = 0$. The immediate result of 'switching on' the damage model is the creation of a heavily damaged ice shelf (with $D \sim 0.5$). Over time, this weaker ice shelf results in the grounding line retreating over more than 100 km. At the same time spots of intense damage ($D \sim 0.9$) generated where the grounding line crosses the channel walls around x = 500 km and y = {10, 70} km are transported downstream, to form strips that extend to the calving front.

The Cryosphere Discuss., doi:10.5194/tc-2017-53, 2017
Manuscript under review for journal The Cryosphere
Discussion started: 3 April 2017

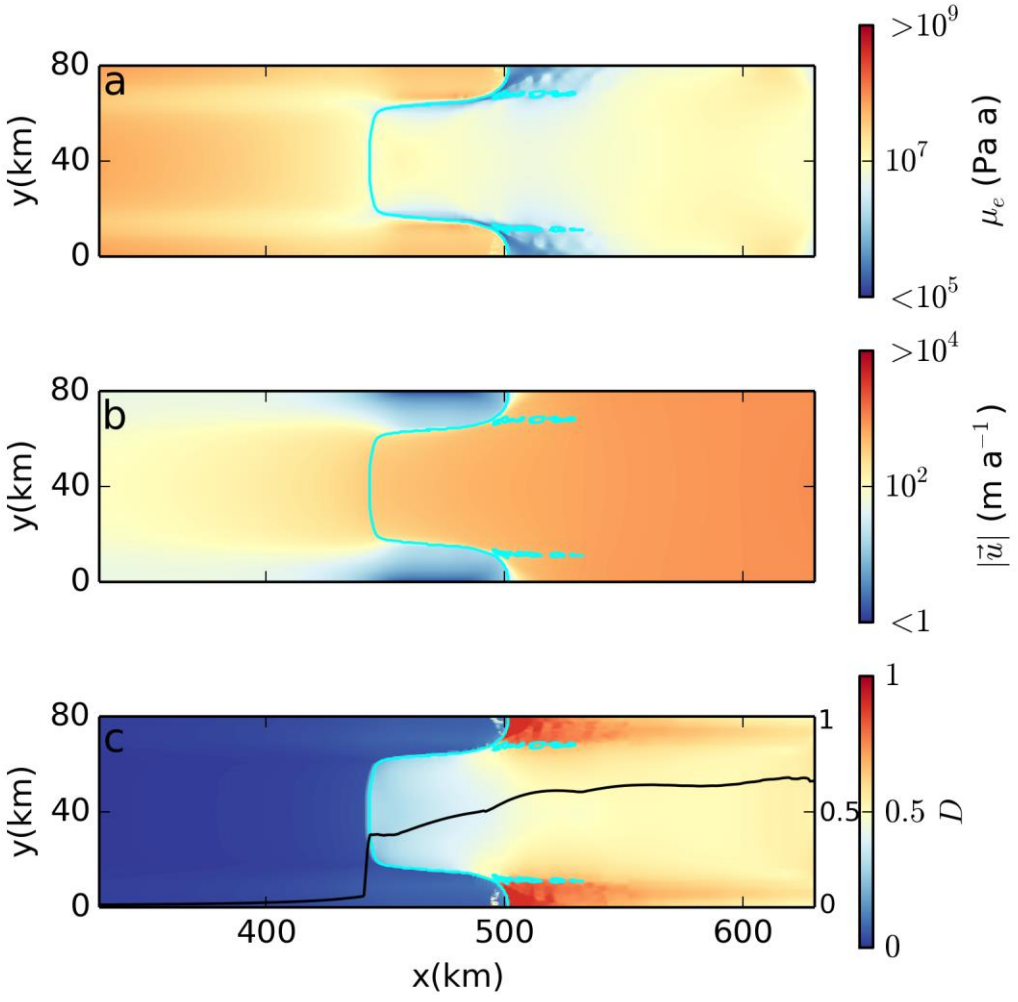

Figure 2: Initial variables in experiment IceD0: effective viscosity (a), ice velocity (b), damage distribution (c), and grounding line location (shown in cyan on all panels). The black curve in the bottom subfigure is the damage value in the centre of the channel (The scale of D is to the right).

The Cryosphere Discuss., doi:10.5194/tc-2017-53, 2017
Manuscript under review for journal The Cryosphere
Discussion started: 3 April 2017

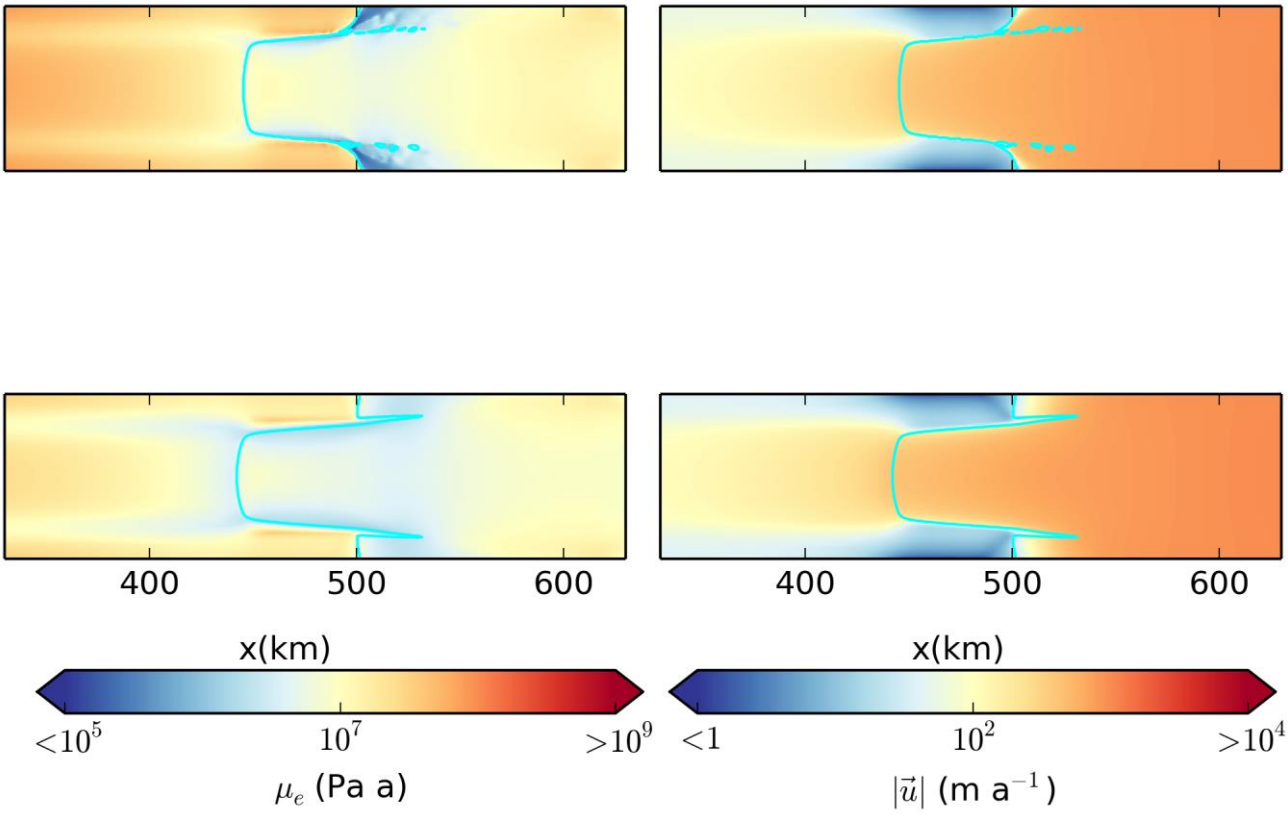

Figure 3: Comparison of the Ice0 (upper panel) and IceD0 (lower panel) patterns of effective viscosity and velocity at the end of the 1000 year simulations. These are approximately steady state patterns as the grounded area and volumes change very little after 1000 years (Figs 6 and 7).

The Cryosphere Discuss., doi:10.5194/tc-2017-53, 2017
Manuscript under review for journal The Cryosphere
Discussion started: 3 April 2017

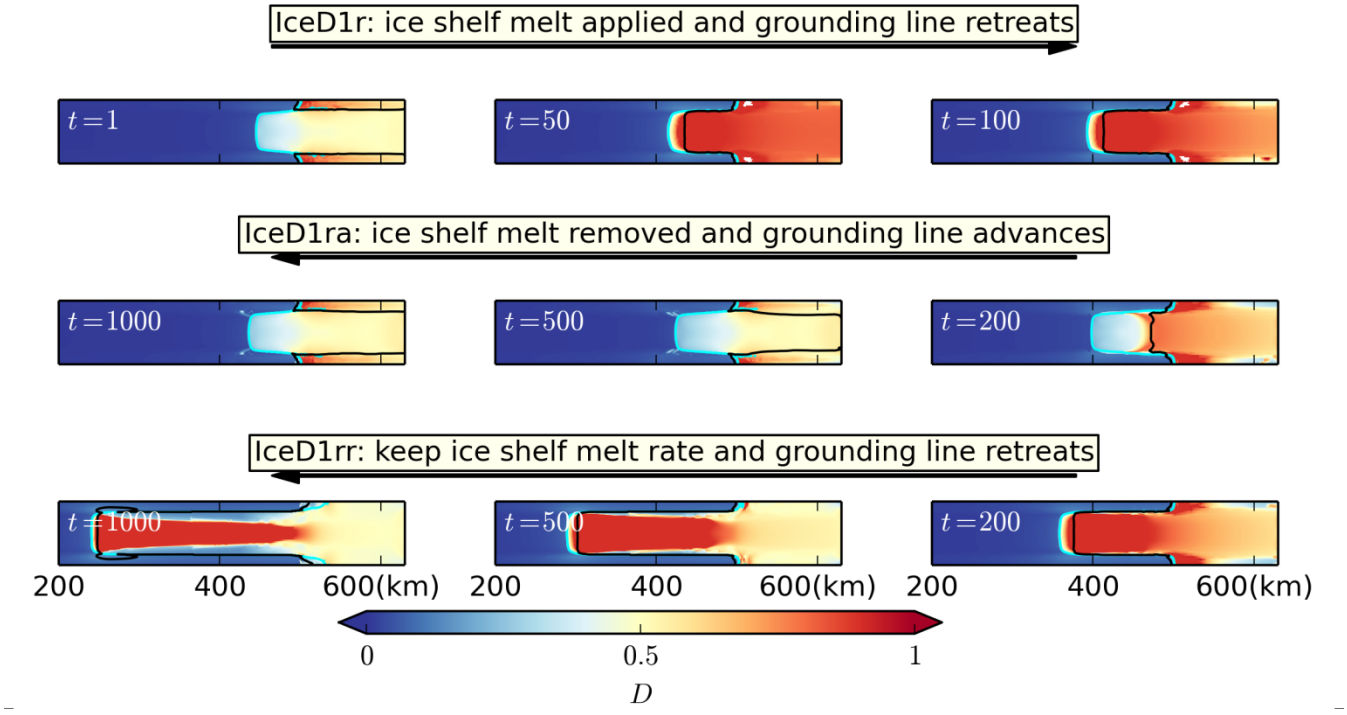

Figure 4: Comparison of the retreat and recover speed due to changes in shelf basal melt forcing (IceD1rr and IceD1ra) in MISMIP+. We show *h*=200 m (black) contours. The grounding line is shown in cyan.

The Cryosphere Discuss., doi:10.5194/tc-2017-53, 2017
Manuscript under review for journal The Cryosphere
Discussion started: 3 April 2017

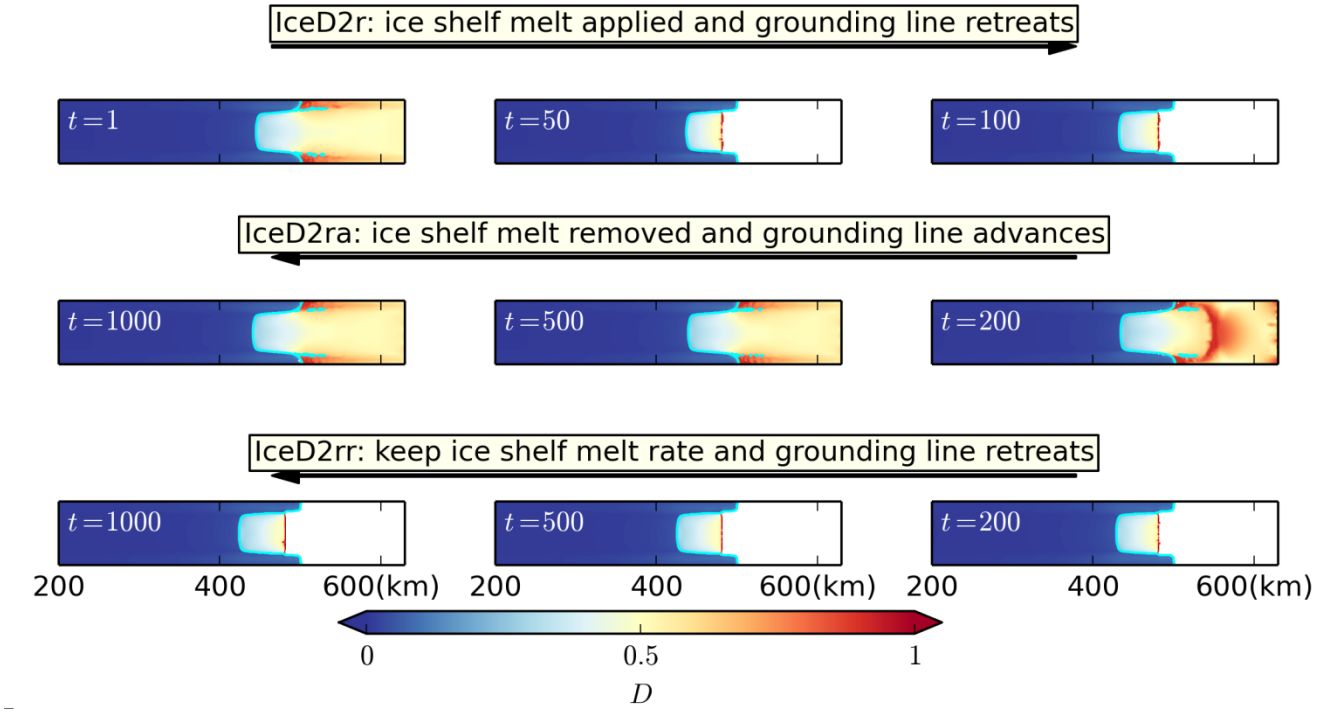

Figure 5: Compare the retreat and recover speed from calving (IceD2rr and IceD2ra) in MISMIP+.

The Cryosphere Discuss., doi:10.5194/tc-2017-53, 2017
Manuscript under review for journal The Cryosphere
Discussion started: 3 April 2017

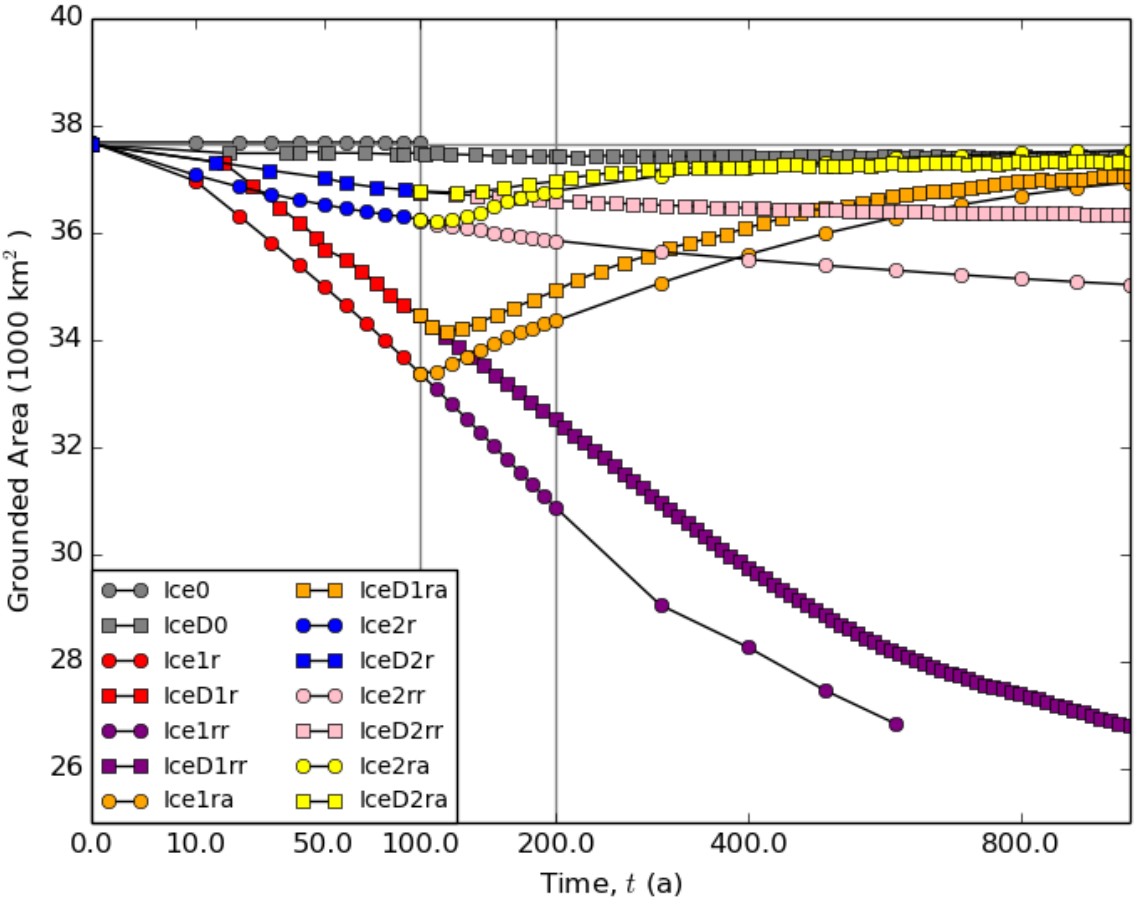

Figure 6: Grounded area against time for all of the simulations. Lines with circles show the results based on BISICLES without the damage model and those with squares show the results based on BISICLES with the damage model. Grey curves show the results of the control run Ice0, IceD0; red curves show the results of Ice1r, IceD1r; orange curves show the results of Ice1ra, IceD1ra; purple curves show the results of Ice1rr, IceD1rr; blue curves show the results of Ice2r, IceD2r; yellow curves show the results of Ice2ra; IceD2ra; pink curves show the results of Ice2rr, IceD2rr.

The Cryosphere Discuss., doi:10.5194/tc-2017-53, 2017
Manuscript under review for journal The Cryosphere
Discussion started: 3 April 2017

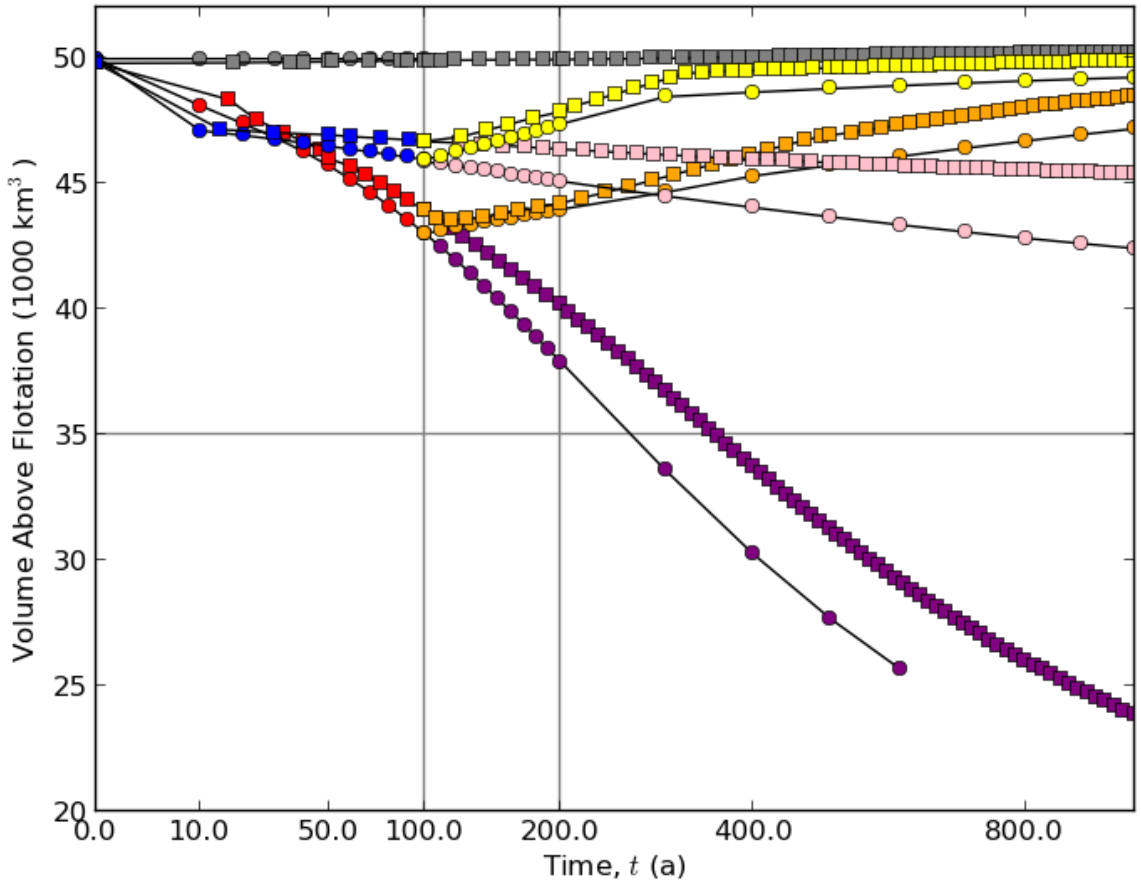

Figure 7: As that for Figure 6 but for volume above flotation.

The Cryosphere Discuss., doi:10.5194/tc-2017-53, 2017
Manuscript under review for journal The Cryosphere
Discussion started: 3 April 2017

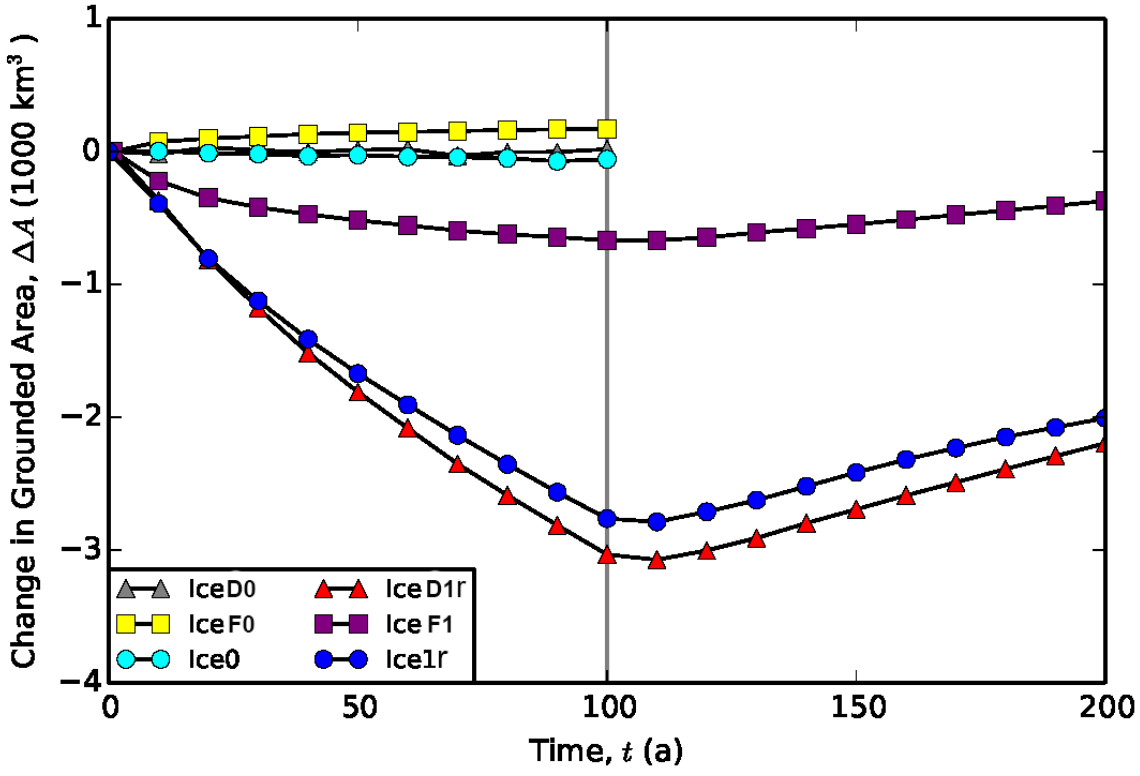

Figure 8: Grounded area against time for the Ice0 and Ice1 experiments with no damage model (Ice0, Ice1r) and the damage model of Sect. 2.2 (IceD0, IceD1r) compared to a simulation where the damage field does not evolve with time but is taken from the initial state of IceD0 (IceF0, IceF1).

The Cryosphere Discuss., doi:10.5194/tc-2017-53, 2017
Manuscript under review for journal The Cryosphere
Discussion started: 3 April 2017

Experiment	Model	Viscous Parameter	Ocean forcing (1-100 year)	Ocean forcing (100-1000 year)
Ice0	BISICLES	A	0	0
Ice1ra	BISICLES	A	Melting	0
Ice1rr	BISICLES	A	Melting	Melting
Ice2ra	BISICLES	A	"Calving"	0
Ice2rr	BISICLES	A	"Calving"	"Calving"
IceD	BISICLES_D	A	0	0
IceD0	BISICLES_D	A'	0	0
IceD1ra	BISICLES_D	A'	Melting	0
IceD1rr	BISICLES_D	A'	Melting	Melting
IceD2ra	BISICLES_D	A'	"Calving"	0
IceD2rr	BISICLES_D	A'	"Calving"	"Calving"
IceF0	BISICLES-Fixeddamage	A'	0	0
IceF1	BISICLES-Fixeddamage	A'	Melting	0

Table 1: Summary of simulations carried out in the current study. The entries in the first column correspond to MISMIP+ experiment names (Asay-Davis et al., 2016).